THE ANNALS OF "DUNĂREA DE JOS" UNIVERSITY OF GALATI
FASCICLE III, 2020, VOL. 43, NO. 1, ISSN 2344-4738, ISSN-L 1221-454X
ELECTROTECHNICS, ELECTRONICS, AUTOMATIC CONTROL, INFORMATICS
Article DOI: https://doi.org/10.35219/eeaci.2020.1.04

INTEGRATION OF PHOTOVOLTAIC SYSTEMS IN A LOW VOLTAGE ELECTRICAL GRID

Alexandru Dușa*[1]

[1] *"Dunărea de Jos" University of Galați, Romania*
[*] *Corresponding author: e-mail: alexandru.dusa@ugal.ro*

Abstract: This paper proposes the connection of photovoltaic panels to the grid by using an active power filter (APF) to reduce harmonics in the electrical system and inject the excess of electricity into the electrical grid. A boost converter was used to raise the voltage to the level imposed by the APF. The APF control was performed by the indirect method and for the extraction of the maximum power from the photovoltaic panels the *Perturb and Observe control algorithm* was used. The design and simulation of the performed system was done within Matlab/Simulink environment. The simulation was performed considering two hypotheses: injection of a higher and lower power than the one absorbed by the nonlinear load connected to the system. This paper considers the possibility of using a unified system which offers the possibility of both injecting electricity from renewable sources into the network and improving the quality of electricity.

Keywords: renewable sources, photovoltaic power station, active power filter, energy quality.

1. INTRODUCTION

The increase of electricity demand and the depletion of fossil fuels in the last decade have led to the use of renewable energy sources, such as photovoltaic panels, due to the cost reductions and technological progress. The connection of photovoltaic panels to the grid is done with the help of power inverters that produce harmonic currents and can increase the Total Harmonic Distortion (*THD*) of the voltage and the current at the common connection point (*CCP*) (Tobnaghi & Vafaei, 2016), (ElNozahy & Salama, 2013). Electrical grids are affected by the diversification of non-linear types of consumers due to the technological progress. These non-linear loads generate harmonics, create imbalances and consume reactive energy. Connecting photovoltaic systems to the electrical grid, which is already affected by harmonics from non-linear loads, will influence the electricity quality (Kalbat, 2013). To fix the problems related to the electricity quality, it is proposed to use a parallel Active Power Filter, which provides good compensation of current harmonics (Bălănuță, 2012). The control algorithm of the Active Power Filter is performed using the indirect control method (Rosu, et al., 2009). The integration of photovoltaic panels in the electrical grid is done through the Active Power Filter, using a boost converter, controlled by the MPPT (Maximum Power Point Tracking) Perturb and Observe (P&O) algorithm, which allows the coupling of photovoltaic panels to the inverter of APF. Thus, a unified system that allows the injection

of electricity into the grid from photovoltaic panels and filtering the harmonics generated by non-linear loads is built (Bouzelata, et al., 2015), (Kannan & Rengarajan, 2013), (Djeghader, et al., 2018).

2. THE UNIFIED SYSTEM

Fig.1 presents the block diagram of the unified system, which allows the injection of electricity into the grid from the photovoltaic panels and the filtering of the harmonic level.

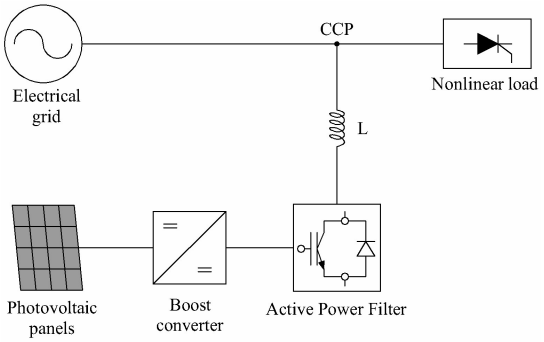

Fig.1. Block diagram of the unified system

2.1. The electrical grid

In this paper, the electrical grid was defined by a three-phase voltage source with an effective line value of 400 V.

2.2. The non-linear load

For the construction of the non-linear load (Fig.2) that generates harmonics in the electrical grid, an uncontrolled rectifier that supplies a load, R = 30 Ω, was used.

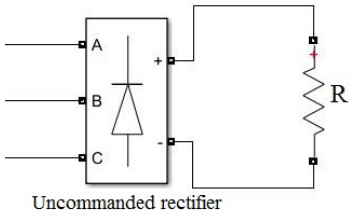

Fig.2. The non-linear load

2.3. The photovoltaic panels

The photovoltaic panels of the Sunerg Solar Energy XM72/156-355I + (IB) ** model were used, having the following characteristics (Table 1).

Table 1 Technical characteristics of the photovoltaic panel

Data	Value	Unit
Open-circuit Voltage (V_{oc})	47.88	V
Voltage at P_{max} (V_{mp})	40.75	V
Short-circuit current (I_{sc})	9.51	A
Current at P_{max} (I_{mp})	8.76	A
V_{oc} Temperature coefficient	-0.3055	%/K
I_{sc} Temperature coefficient	0.0455	%/K
Peak Power (P_{max})	355	W
Number of cells	72	

To perform the simulations in Matlab/Simulink, 50 photovoltaic panels were used, connected in series of 10 panels each to increase the voltage and respectively in parallel to increase the current. Due to the constant changes of the meteorological conditions, it was proposed to define as a test the solar irradiation (Ir) and the temperature (T), for the presentation of two different situations, represented in Table 2.

Table 2 Characteristics of photovoltaic panels depending on solar radiation

Data		Tension [V]	Current [A]	Power [W]
Ir	1000 [W/m^2]	407.5	43.8	17850
T	25 [°C]			
Ir	300 [W/m^2]	395.2	13.16	5202
T	25 [°C]			

In order to implement the photovoltaic park in Matlab/Simulink, the "*PV* array" block was used (Fig.3). It allows the modeling of a variation of photovoltaic panels using the technical data of the desired panels.

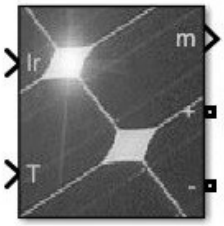

Fig.3. Block "*PV* array"

Fig.4 presents the curve indicating the maximum power point as a function of solar radiation for the defined photovoltaic park.

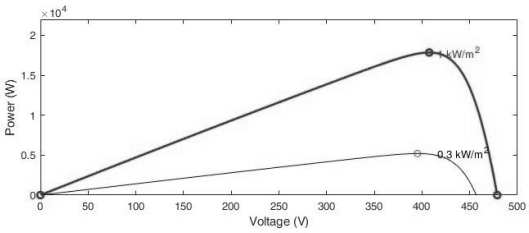

Fig.4. Maximum power curve depending on solar radiation

2.4. The boost converter

The boost converter has a higher output voltage than the *DC* input voltage. Fig.5 presents the wiring diagram of the boost converter made in Matlab/Simulink. It operates as follows: when the *IGBT* (Insulated Gate Bipolar Transistor) is closed, the coil is charged from the photovoltaic panels and stores electricity. The diode blocks the current that is supplied due to the discharge of the capacitor; when the IGBT tarnzistor is open, the energy stored in the coil charges the capacitor (Singh & Kundu, 2020), (Erickson & Maksimovic, 2004).

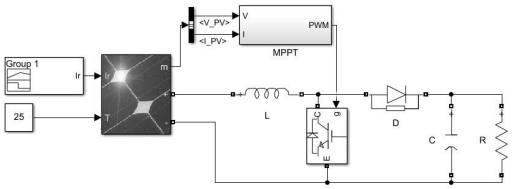

Fig.5. The boost converter

Design of the boost converter

Determination of input power P_{in}:

$$(1) \quad P_{in} = V_{in} \cdot I_{in}$$

where V_{in} – input voltage, I_{in} – input current.

It is assumed that the efficiency of the converter will be at least η = 90%. Using equation (2) it can be calculated the output power P_{out}.

$$(2) \quad P_{out} = P_{in} \cdot \eta$$

The output current I_{out} is the following:

$$(3) \quad I_{out} = \frac{P_{out}}{V_{out}}$$

where: V_{out} is the output voltage.

The resistance R simulating the load is given by the equation (4). It allows the determination of the parameters of the boost converter.

$$(4) \quad R = \frac{V_{out}^2}{P_{out}}$$

The duty cycle D depends on the input and output voltage - equation (5).

$$(5) \quad D = -\left(\frac{V_{in}}{V_{out}} - 1\right)$$

The time T of a period is

$$(6) \quad T = \frac{1}{f}$$

where: f – switching frequency.

Transient time t_{on}:

$$(7) \quad t_{on} = D \cdot T$$

Determination of the coil L

The average current through the coil I_L is calculated with the equation (8).

$$(8) \quad i_L = \frac{I_{out}}{1 - D}$$

Current loss through the coil Δi_L must be at most 10%.

$$(9) \quad \Delta i_L = i_L \cdot 10\%$$

The coil is calculated with equation (10). The value of the coil obtained to meet the requirements must be greater than about 20%.

$$(10) \quad L = \frac{V_{in} \cdot t_{on}}{\Delta i_L}$$

Determination of the capacitor C

Voltage losses ΔV_c must be less than 1%.

$$(11) \quad \Delta V_c = V_{out} \cdot 1\%$$

The value of the capacitor C is determined by the equation (12).

$$(12) \quad C = \frac{I_{out} \cdot t_{on}}{\Delta V_c}$$

Values used for sizing the boost converter

Table 3 presents the values used for sizing the boost converter.

Table 3 Values boost converter

Data	Value	Unit
Coil (*L*)	2	mH
Condenser (*C*)	58	μF
Resistance (*R*)	31.5	Ω
Frequency IGBT (*f*)	25	kHz

Converter control algorithm

Photovoltaic systems can produce maximum power when operate at a single point, maximum power point (*MPP*). Aiming to operate at this point, photovoltaic systems contain a MPPT (Maximum Power Point Tracking) controller that monitors the maximum power point.

In this paper, the MPPT controller uses the Perturb and Observe (P&O) control algorithm to optimize the power from the photovoltaic system (Karami, et al., 2017), (Safari & Mekhilef, 2011). The control algorithm is represented in Fig.6.

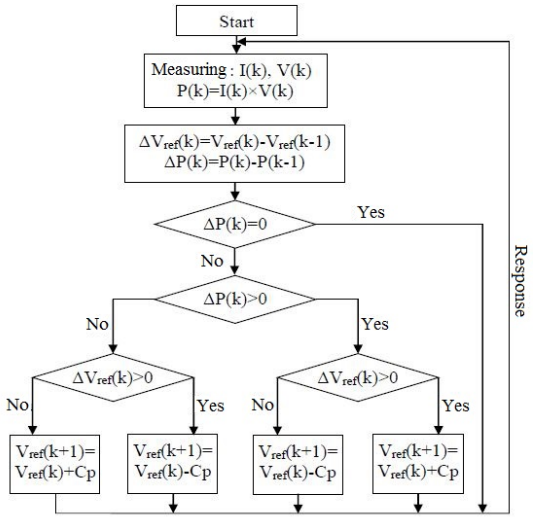

Fig.6. Control algorithm P&O

2.5. Active Power Filter

Indirect control is a strategy that does not require knowledge about the current spectrum followed by unbalanced load and reactive current (Rosu, et al., 2009).

$$(13) \qquad i_{sa}(t) = i_{La}(t) + i_{fa}(t)$$

The electric current on the phase *a* absorbed by the nonlinear load is:

$$(14) \qquad i_{La}(t) = i_{La}^{1}(t) + \sum_{k} i_{Lak}(t) + i_{Laq}(t)$$

where:

$i_{La}^{1}(t)$ - the active component of the fundamental;

$\sum_{k} i_{Lak}(t)$ - the sum of the higher harmonics;

$i_{Laq}(t)$ - the reactive component of the fundamental.

The electric current through the filter will be:

$$(15) \qquad i_{fa}(t) = i_{fa}^{1}(t) + \tilde{i}_{fa}(t)$$

where:

$i_{fa}^{1}(t)$ - has the same meaning as $i_{La}^{1}(t)$;

$\tilde{i}_{fa}(t)$ represents the harmonic component of the filtered electric current.

The current absorbed by the grid must be sinusoidal and must have the same phase as the voltage. The component to be compensated by the active filter is given by:

$$(16) \qquad \tilde{i}_{fa}(t) + \sum_{k} i_{Lak}(t) + i_{Laq}(t) = \tilde{i}(t)$$

From the equations (13) - (16) it results:

$$(17) \qquad i_{sa} = i_{La}^{1} + i_{fa}^{1} + \tilde{i}$$

The signal is generated as a setpoint for the current controller on the phase *a* of the power supply:

$$(18) \qquad i_{a}^{*}(t) = \varepsilon_{DC} \frac{v_a}{\sqrt{2}V} = \varepsilon_{DC} \sin \omega t$$

where:

V is the effective value of the supply phase voltage, and ε_{DC} - the output of the voltage controller on the capacitance *C* of the converter.

The above charge is compared with the measured value of the electric current absorbed from the grid, i_{sa}, resulting for the control of the filter on the phase *a*:

$$(19) \qquad u_{ca}^{*} = k(i_{a}^{*} - i_{sa}) = k(i_{a}^{*} - \tilde{i} - i_{La}^{1} - i_{fa}^{1})$$

where: *k* is the amplification of the controller.

Since the regulator is linear, the sinusoidal components of the load and the filter are obviously found in the sinusoidal setpoint of the controller:

$$(20) \qquad i_{a}^{*} = i_{La}^{1} + i_{fa}^{1}$$

With this remark results that the setpoint for the phase *a* of the active filter becomes:

$$u_{ca}^{*} = -k\tilde{i} = -k\left(\tilde{i}_{fa}(t) + \sum_{k} i_{Lak}(t) + i_{Laq}(t)\right) \quad (21)$$

that is proportional to the polluting component. If it is correctly designed in steady state, the controller cancels the stationary error at the input:

$$\tilde{i}_{fa}(t) = -\left(\sum_{k} i_{Lak}(t) + i_{Laq}(t)\right) \quad (22)$$

so, the filter will generate the polluting component itself necessary to the nonlinear load.

The setpoint of ε_{DC} on the RV_{DC} controller for charging capacitor C is converted to the current reference:

$$\begin{cases} i_a^{*} = \varepsilon \cdot \sin \omega t \\ i_b^{*} = \varepsilon \cdot \sin(\omega t - 2\pi/3) \\ i_c^{*} = \varepsilon \cdot \sin(\omega t - 4\pi/3) \end{cases} \quad (23)$$

Hysteresis controllers with a control band correlated with the maximum allowed switching frequency and the desired performances or classic *PI* type regulators can be used for current control.

The sinusoidal functions are obtained by *PLL* loop and voltage acquisition. Thus, the zero-current flow of the unbalanced load will be done through APF.

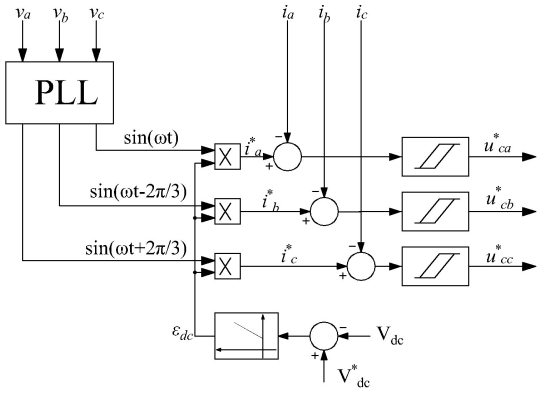

Fig.7. Indirect Control

Values used for sizing the Active Power Filter

Table 4 presents the values used to size the Active Power Filter.

Table 4 Active Power Filter Values

Data	Value	Unit
Line voltage (U_L)	400	V
Filtration inductance (L)	2.4	mH
Storage capacity (C)	2000	μF
Continuous voltage of the APF (U_{cc})	750	V

3. SIMULATION AND RESULTS

In this paper it was proposed to inject renewable energy through the Active Power Filter, while filtering the harmonics generated by the nonlinear load. It takes into account two hypotheses depending on solar radiation (*Ir*). The simulations were performed in Matlab/Simulink (Fig.8).

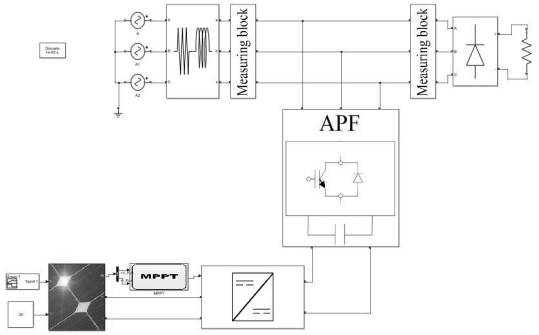

Fig.8. Unified system implementation scheme in Matlab/Simulink

Fig.9 presents the waveform of the supply voltage and the current absorbed by the nonlinear load on phase *a*.

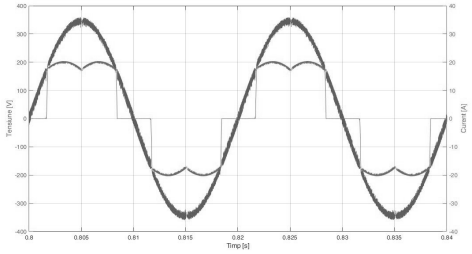

Fig.9. Waveform voltage and current of the nonlinear load on the phase *a*

The harmonic level generated by the non-linear load is presented in Fig.10, *THDi* = 30.08%.

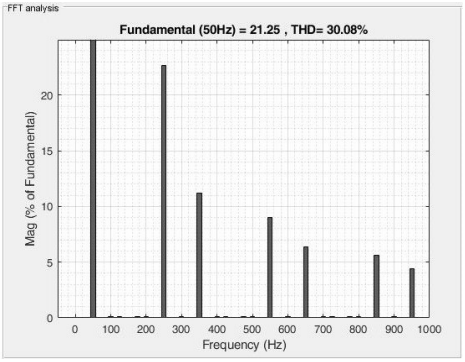

Fig.10. FFT analysis of the current waveform for non-linear load

In the first case, for the solar radiation (*Ir*) the value of 1000W/m^2 was imposed, which allows the operation of photovoltaic panels at maximum power (P_{max}). Fig.11 presents the waveform of the supply voltage and the waveform of the current injected into the grid on the phase a. In this case, the photovoltaic panels produce more power than the demand for the non-linear load and the excess electricity is injected into the grid.

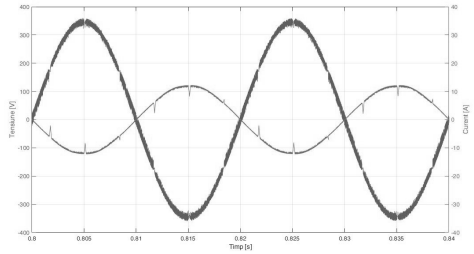

Fig.11. The waveform of the voltage and current injected into the grid on the phase *a*

After making the *FFT* (Fast Fourier Transformation) analysis (Fig.12) of the waveform of the current on the phase *a* injected in the grid it resulted *THDi* = 5.34%.

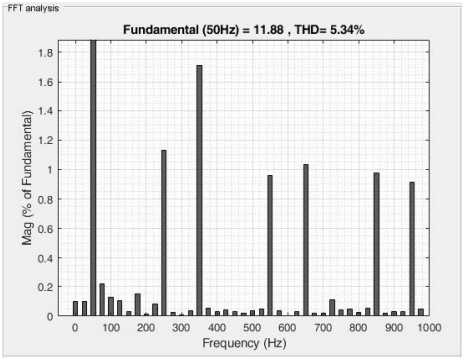

Fig.12. FFT analysis of the current waveform in the first hypothesis

Fig.13 presents the compensation current generated by the photovoltaic system through the Active Power Filter.

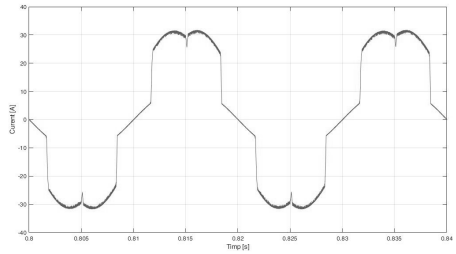

Fig.13. The waveform of the current generated by *PV* through *APF* in the first hypothesis

In the second hypothesis, for the solar irradiation (*Ir*) was imposed the value of 300W/m^2, which makes the photovoltaic system to generate less power. Fig.14 presents the waveform of the supply voltage and the waveform of the main current on the phase *a*. In this case, the photovoltaic panels produce less power than the demand for the nonlinear load and the grid provides some electricity to the nonlinear load.

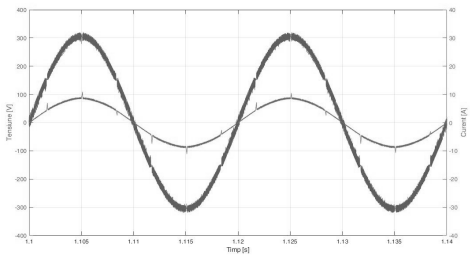

Fig.14. Voltage and current waveform in case of less power produced by *PV*

FFT analysis (Fig.15) of the current waveform on the phase 1 in case of generating a power lower than the nonlinear load of the photovoltaic system is *THDi* = 4.33%.

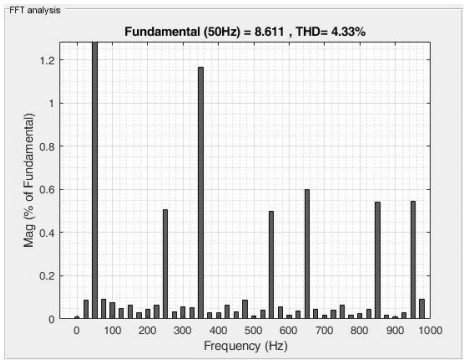

Fig.15. *FFT* analysis of the current waveform in hypothesis two

Fig.16 presents the compensation current generated by the photovoltaic system through the Active Power Filter.

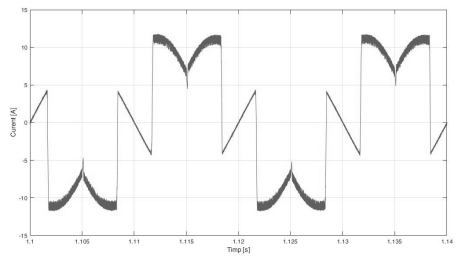

Fig.16. The waveform of the current generated by *PV* through *APF* in hypothesis two

Fig. 17 presents the variable transition regime from the permanent regime when the photovoltaic panels produce a power depending on the solar irradiation *Ir* = 1000W/m^2 to the permanent regime when the solar irradiation *Ir* = 300W/m^2.

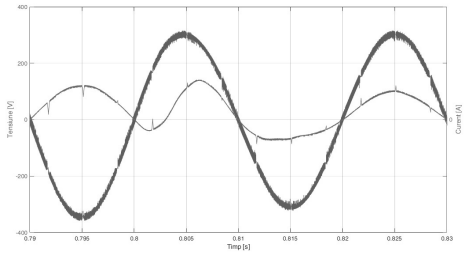

Fig. 17. Transitory regime

4. CONCLUSIONS

This paper presents a unified system that allows the injection of renewable energy produced by photovoltaic systems into the electricity grid and the filtering of harmonics generated by non-linear loads.

This is done analyzing two hypotheses:

I. The photovoltaic system produces a higher power than that absorbed by the non-linear load and the excess electricity is injected into the electricity grid, while reducing the harmonics generated by the nonlinear load to *THDi* = 5.34%.

II. The photovoltaic system produces less power than that absorbed by the non-linear load and the electrical grid supplies some of the electricity to the non-linear load, while reducing the harmonics generated by the non-linear load at *THDi* = 4.33%.

In this paper the performance of such a unified system that offers in the future the injection of renewable energy into the electricity grid and the improvement of electricity quality is determined.

5. ACKNOWLEDGMENT

This study was supported by the CRESC-INTEL project „*Knowledge Transfer Regarding the Energy Efficiency Increase and Intelligent Power Systems*" code SMIS 105803, project co-funded by the European Union from the European Regional Development Fund through the Competitiveness Operational Program 2014-2020.

6. REFERENCES

Bălănuță, C. D., 2012. Cercetări și contribuții privind îmbunătățirea calității energiei electrice în sistemele electrice. Galați, s.n. Doctoral thesis.

Bouzelata, Y., Kurt, E., Altın, N. & Chenni, R., 2015. Design and simulation of a solar supplied multifunctional active power filter and a comparative study on the current-detection algorithms. *Renewable and Sustainable Energy Reviews*, pp. 1114-1126.

Djeghader, Y., Chelli, Z. & Rehaimia, S., 2018. Harmonic Mitigation in Electrical Grid Connected Renewable Energy Sources. *ACTA Electrotehnica* 59(4), pp. 287-291.

El Nozahy, M. S. & Salama. M. M. A., 2013. Technical impacts of grid-connected photovoltaic systems on electrical. *Journal of renewable and sustainable energy 5*, Issue doi: 10.1063/1.4808264, pp. 1-11.

Kalbat, A., 2013. PSCAD Simulation of Grid-Tied Photovoltaic Systems and Total Harmonic Distortion Analysis. *2013 3rd International Conference on Electric Power and Energy Conversion Systems*, doi:10.1109/EPECS.2013.6713002

Kannan, V. K. & Rengarajan, N., 2013. Control of Photovoltaic System with A DC-DC Boost Converter Fed DSTATCOM Using Icos Algorithm. *Journal of Applied Science and Engineering*, 16(1), pp. 89-98.

Karami, N., Moubayed, N. & Outbib, R., 2017. General review and classification of different MPPT Techniques. *Renewable and Sustainable Energy*, 68(1), pp. 1-18.

Rosu, E., Culea, M., Dumitriu. T., Munteanu, T. & Paduraru. R., 2009. Active Power Filter with Indirect Control for Line-Frequency Controlled Rectifiers. *The ANNALS of "Dunărea de Jos" University of Galati*, 32(1), pp. 30-36.

Safari, A. & Mekhilef, S., 2011. Simulation and Hardware Implementation of Incremental Conductance MPPT With Direct Control Method Using Cuk Converter. *IEEE Transactions on Industrial Electronics*, 58(4), pp. 1154-1161.

Singh, G. & Kundu, S., 2020. An efficient DC-DC boost converter for thermoelectric energy harvesting. *International Journal of Electronics and Communications (AEÜ)*, 118, pp. 1-10.

Erickson, R. W. & Maksimovic, D., 2004. *Fundamentals of Power Electronics*. ISBN 978-1-4757-0559-1 ed. Norwell, Massachusetts 02061 USA: Electronic Services

Tobnaghi, D. M. & Vafaei, R., 2016. The impacts of grid-connected photovoltaic system on distribution networks- a review. *ARPN Journal of Engineering and Applied Sciences*, 11(5), pp. 3564-3570.